Research papers

Sediment entrainment into sea ice and transport in the Transpolar Drift: A case study from the Laptev Sea in winter 2011/2012

C. Wegner[a], K. Wittbrodt[b], J.A. Hölemann[c,*], M.A. Janout[c], T. Krumpen[c], V. Selyuzhenok[c], A. Novikhin[d], Ye. Polyakova[e], I. Krykova[f], H. Kassens[a], L. Timokhov[d]

[a] GEOMAR Helmholtz Centre for Ocean Research, Kiel, Germany
[b] Christian-Albrechts University, Kiel, Germany
[c] Alfred Wegener Institute, Helmholtz Centre for Polar and Marine Research, Bremerhaven, Germany
[d] State Research Center – Arctic and Antarctic Research Institute, St. Petersburg, Russia
[e] Lomonosov Moscow State University, Moscow, Russia
[f] P.P.Shirshov Institute of Oceanology, Russian Academy of Sciences, Moscow, Russia

ARTICLE INFO

ABSTRACT

Sea ice is an important vehicle for sediment transport in the Arctic Ocean. On the Laptev Sea shelf (Siberian Arctic) large volumes of sediment-laden sea ice are formed during freeze-up in autumn, then exported and transported across the Arctic Ocean into Fram Strait where it partly melts. The incorporated sediments are released, settle on the sea floor, and serve as a proxy for ice-transport in the Arctic Ocean on geological time scales. However, the formation process of sediment-laden ice in the source area has been scarcely observed.

Sediment-laden ice was sampled during a helicopter-based expedition to the Laptev Sea in March/April 2012. Sedimentological, biogeochemical and biological studies on the ice core as well as in the water column give insights into the formation process and, in combination with oceanographic process studies, on matter fluxes beneath the sea ice. Based on satellite images and ice drift back-trajectories the sediments were likely incorporated into the sea ice during a mid-winter coastal polynya near one of the main outlets of the Lena River, which is supported by the presence of abundant freshwater diatoms typical for the Lena River phytoplankton, and subsequently transported about 80 km northwards onto the shelf. Assuming ice growth of 12–19 cm during this period and mean suspended matter content in the newly formed ice of 91.9 mg l^{-1} suggests that a minimum sediment load of 8.4×10^4 t might have been incorporated into sea ice. Extrapolating these sediment loads for the entire Lena Delta region suggests that at least 65% of the estimated sediment loads which are incorporated during freeze-up, and up to 10% of the annually exported sediment load may be incorporated during an event such as described in this paper.

1. Introduction

Arctic Ocean sea ice extent and thickness, as well as volume and age of multiyear ice has decreased over the last 20 years (e.g. Serreze et al., 2007; Maslanik et al., 2007; Comiso et al., 2008; Mahoney et al., 2008; Kwok et al., 2009). This decrease is concurrent with an increase in the Arctic sea ice drift speed of about 10% decade^{-1} with the strongest increase after 2004 (46% decade^{-1}; Spreen et al., 2011). With decreasing ice coverage and the recent high sea ice export through Fram Strait, the annual sea ice export increased by 5% (Smedsrud et al., 2011). A substantial part of the sea ice found in Fram Strait is assumed to be formed on the Siberian shelf seas, in particular in the Laptev Sea as the most important region for sea-ice production and

export (Krumpen et al., 2013). Generally sea ice serves as an important vehicle for sediment transport in the Arctic Ocean (e.g. Polyak et al., 2010; Darby et al., 2011). In particular on the Laptev Sea shelf, sediments are incorporated into newly formed ice during autumn freeze-up (e.g. Eicken et al., 1997, Wegner et al., 2005) and transported across the Arctic Ocean via the Transpolar Drift toward Fram Strait and the East Greenland shelf, where the ice melts and releases the material into the water column (e.g. Reimnitz et al., 1994; Dethleff et al., 2000, Eicken et al., 1997, 2000). The Laptev Sea shelf is ice covered from mid-October until June and features fast ice, flaw polynyas, and drift ice (Bareiss and Görgen, 2005). Fast ice covers more than 50% of the shallow eastern Laptev Sea shelf and up to 25% of the western Laptev Sea (Bareiss and Görgen, 2005). Its extent roughly coincides with the

---

* Correspondence to: Alfred Wegener Institute for Polar and Marine Research, Am Handelshafen 12, 27570 Bremerhaven, Germany.
  E-mail address: jens.hoelemann@awi.de (J.A. Hölemann).

position of the 20 m isobath (Bareiss and Görgen, 2005). Polynyas are open water regions that develop north of the landfast ice edge during offshore-directed winds (Bareiss and Görgen, 2005). Mean polynya areas in the central Laptev Sea range from 20×10^3 km^2 in May to 90×10^3 km^2 in July (Bareiss and Gören, 2005). The largest polynya with an area of 4×10^3 km^2 in winter is the West New Siberian Polynya (Zakharov, 1966; Bareiss and Görgen, 2005). Sediment entrainment processes on the vast Siberian shelf seas are assumed to be most effective during the autumn freeze-up (Eicken et al., 2005; Wegner et al., 2005) in water depth less than 20 m (e.g. Kempema et al., 1989; Sherwood, 2000). Previous studies suggested that suspension freezing also takes place in polynyas in late-winter in water depths between 20 and 30 m (e.g. Dethleff, 2005). Sediments are generally incorporated into sea ice by two entrainment processes: primarily by suspension freezing in frazil ice (e.g. Reimnitz et al., 1992; Eicken et al., 2000; Dethleff and Kempema, 2007) and to a smaller extent by anchor ice entrainment (e.g. Darby et al., 2011). Suspension freezing requires open water to allow for wave activity, bottom currents or wind-driven Langmuir helical cells, leading to resuspension of bottom sediments during episodes of frazil ice formation (e.g. Eicken et al., 2005, Dethleff and Kempema, 2007). Shelf sources in sea-ice samples from the outer Laptev Sea and from Fram Strait were mainly identified based on sedimentological, clay mineralogical and geochemical aspects (e.g. Eicken et al., 1997; Dethleff, 2005; Dethleff and Kuhlmann, 2010). However, only few direct observations of sediment entrainment into sea ice exist from the Siberian shelves (e.g. Hölemann et al., 1999a, 1999b; Lindemann et al., 1999), mainly due to the region's inaccessibility during early and mid-winter.

In the Chukchi and Beaufort Seas, there is evidence for an increase of sediment-laden ice due to an increase in mid-winter landfast ice break-out events (Eicken et al., 2005). In the Laptev Sea, Krumpen et al. (2013) observed a positive trend in sea ice export from the shelf during the last 20 years, likely as a consequence of a thinning and more mobile ice cover. Changes in the amount of sediment-laden ice not only impact the across- and along-shelf transport of suspended particulate matter (SPM), but also the biological productivity in and below the sea ice (e.g. Eicken et al., 2005, Junge et al., 2004) as well as the potential dispersion of pollutants. However, the implications of changing sea ice conditions on the Siberian shelves for sediment entrainment, export and transport across the Arctic Basin are poorly understood.

A helicopter-based Russian-German expedition to the southeastern Laptev Sea in late winter (TRANSDRIFT XX; 19 March – 24 April 2012) provided the rare opportunity to study sediment-laden sea ice by sampling and analyzing ice cores and water column parameters. Biogeochemical, sedimentological and microalgae analysis of the sea ice core are combined with fast-ice based water sampling and remote sensing data to reconstruct the origin and entrainment conditions and discuss the importance of sea ice transport for sediment export from the shelf. In addition a year-round oceanographic mooring "KHATANGA" deployed in the vicinity of the West New Siberian Polynya (Fig. 1) was investigated for potential entrainment processes in the polynya region.

2. Material and method

The ice core was drilled on the fast ice of the inner eastern Laptev Sea shelf (TI12_07; Fig. 1) on 12 April 2012 at air temperatures of −20 °C using an electromechanical ice corer (Kovacs Enterprise, USA) with an inner core diameter of 9 cm. The 1.80 m long sea ice core contained layers with sediment inclusions in the upper parts of the core. The ice core was placed in polyethylene bags and transported frozen to the land-based laboratory in Tiksi. Within several hours after coring the ice core was split into 10 cm long segments, and placed in polyethylene boxes to melt in the dark at room temperature for SPM and colored dissolved organic matter (CDOM) analysis, and at < 4 °C for phytoplankton investigations. Sea ice salinity was determined with

an electrical conductometer (HI 8733, Hanna Instruments).

Complementary water samples were collected during the expedition on the fast ice near the major outlets of the Lena River (TI12_03, TI12_05, TI12_10) and near the fast ice edge of the West New Siberian Polynya (TI12_01, TI12_06, TI12_09). Under-ice seawater for phytoplankton study was sampled with a Niskin water sampler at standard water depths. Wind conditions during sampling varied between 4.9 m s^{-1} at TI12_06 and 12 m s^{-1} from E at TI_12_01 and _02. Atmospheric conditions and climatological reference for mean November-December winds were investigated based on NCEP Reanalysis over the eastern Lena Delta (Fig. 2).

2.1. Quantitative and qualitative SPM analysis

SPM was measured from the ice core and water column samples. For quantitative studies in the water column direct (water sampling) and indirect measurements (turbidity measurements) were carried out. SPM concentrations from water and melted sea ice samples were derived by filtering the samples through pre-weighed filters (MILLIPORE Durapore membrane filters, 0.45 μm pore size) by applying the traditional weighing procedures. A Seapoint turbidity meter connected to a CTD (Conductivity Temperature Depth; SBE19plus, Seabird, USA) was used in order to collect water column turbidity, salinity, and temperature measurements. The turbidity meter emits light of 880 nm wavelength with a sampling rate of 10 Hz. It detects light scattered by particles within the water column and generates an output voltage proportional to particles in the water column, with high backscatter indicating high SPM concentration. The output is given in Formazine Turbidity Unit (FTU), a calibration unit based on formazine as a reference suspension.

Additionally the echo intensity of the upward-looking ADCP (Acoustic Doppler Current Profiler; Workhorse Sentinel 300 kHz, RD-Instruments) deployed at the mooring station Khatanga was used as a relative measure for SPM concentration in the entire water column with increased echo intensity indicating increased SPM concentration (e.g. Gartner and Cheng, 2001, Wegner et al., 2006). ADCP measurements were carried out at intervals of 1 min and averaged over 30 min in 1 m depth bins with the first bin measuring 3 m above bottom. For more information on the Khatanga mooring and data processing please refer to Hölemann et al. (2011) and Janout et al. (2013).

For qualitative studies regarding grain size distribution and SPM composition scanning electron microscope (SEM) measurements with a CamScan-CS-44 were carried out at the REM-laboratory in the Institute of Geosciences at the Christian-Albrechts-University Kiel (Germany) on filtered water (TI_12_06) and sediment-laden sea ice samples (TI_12_07).

2.2. Nutrients

Nutrients were sampled in the water column as well as in sea ice. The sea ice samples were filtered when necessary. The 125 ml samples were added to Nessler cylinders with 35 ml for silicates and with 50 ml for phosphates analysis. 4 ml of a mixed reagent and 1 ml of ascorbic acid were added sequentially to the phosphate samples in order to analyze the samples with a photo-colorimeter FC-3 after a 10-min exposure. 1 ml of a mixed reagent, 1 ml of oxalic and 1 ml of ascorbic acid were added sequentially to the silicate samples to obtain the color. They were analyzed after 30 min' exposition with a photo-colorimeter FC-3. All frozen samples were then transported to the Russian-German Otto Schmidt Laboratory for Polar and Marine Research (OSL) in St. Petersburg and analyzed with an autoanalyzer Skalar Sun Plus System.

2.3. CDOM absorption

Immediately after melting the sea ice samples were subjected to vacuum filtration (with a 250 ml Nalgene filtration set at approx. 400
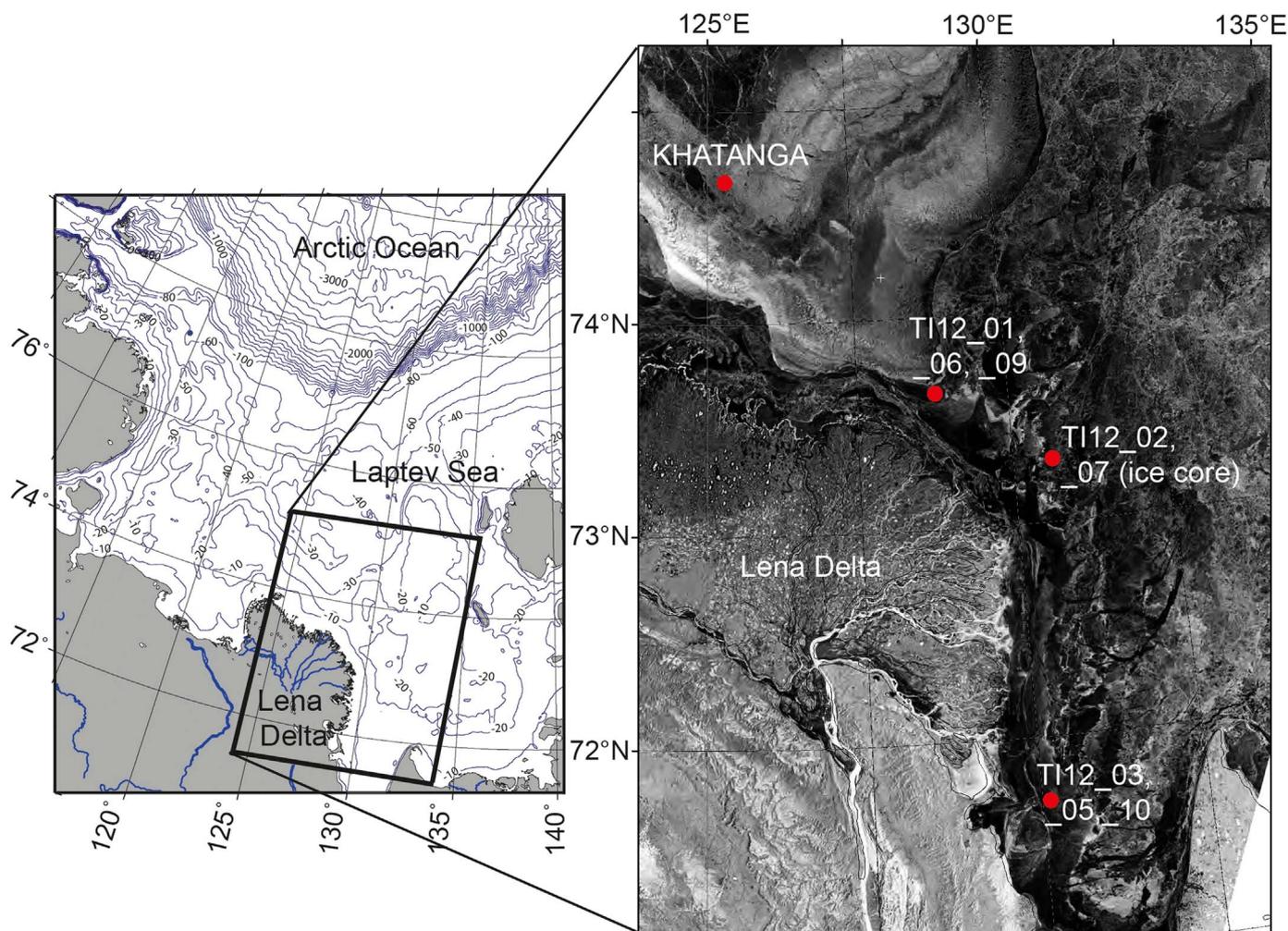
Fig. 1. Bathymetric map of the Laptev Sea. The black rectangle shows the position of the detailed ENVISAT synthetic aperture radar (SAR) scene of the eastern Laptev Sea shelf from April 8, 2012 with the ice coverage of the area, the locations of the presented measuring sites during TRANSDRIFT XX and of the long-term mooring station KHATANGA.
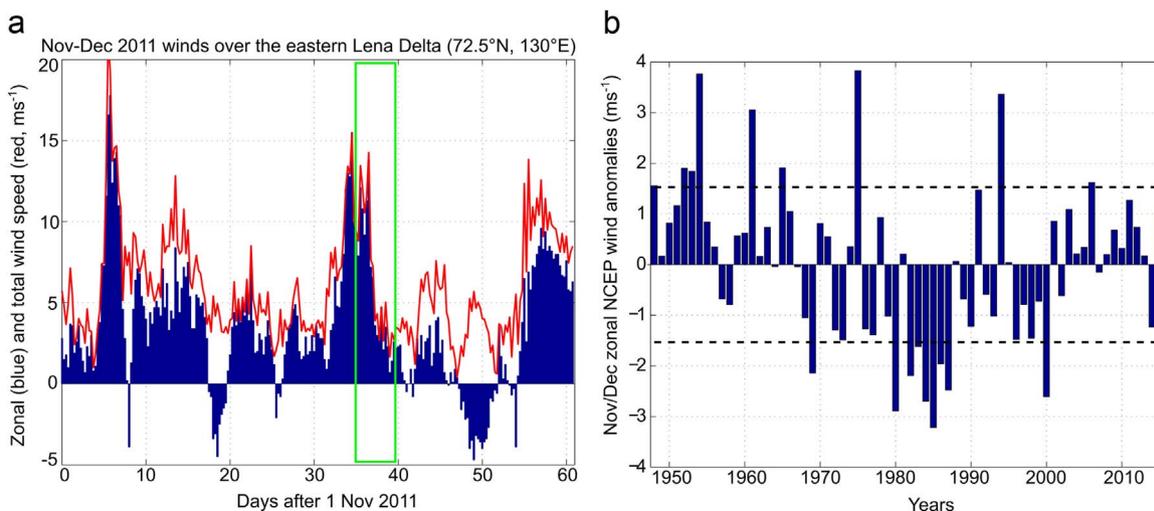
Fig. 2. a) 6-hourly zonal NCEP winds (blue bars) and total wind speed (red line) [m s^{-1}] in November – December 2011 around the assumed entrainment period (green box) over the eastern Lena Delta (72.5°N, 130°E). (b) Mean November-December zonal wind anomalies (blue bars) [m s^{-1}] including one standard deviation (dashed lines). (For interpretation of the references to color in this figure legend, the reader is referred to the web version of this article.)

mbar) through a Whatman GF/F glass microfiber filter (4.7 cm diameter) with a nominal pore size of approx. 0.7 µm. The filter was pre-washed with ~20 ml Milli-Q water and ~ 20 ml of the seawater sample. After washing the filter, 200 ml of seawater was filtered, filled into two storage bottles (high density polyethylene), and stored in a dark and cold environment. CDOM was measured immediately after the expedition at the OSL using a UV/VIS Spectrophotometer (Specord200, analytik jena). Optical Density (OD) spectra of the

filtrates were measured from 300 nm to 750 nm in 1 nm steps using a 10 cm cuvette. Absorption (m^{-1}) was calculated using $2.303 \times OD/0.1$. In this study, we present the CDOM absorption at a wavelength of 375 nm.

2.4. Algae processing and enumeration

The melted sea ice and under-ice seawater samples were filtered through nuclear pore filters (1 μm pore size) at a pressure of < 0.2 bar until 10–30 ml of melt water or seawater remained over the filter. The remaining samples were fixed with neutralized formalin to a final concentration of 4% in the laboratory in Tiksi. Further processing of all samples was carried out at the OSL and the Lomonosov Moscow State University (Geographical Faculty, Scientific-Research Laboratory of Pleistocene Palaeogeography). The algae were washed off the filters by means of a soft brush and re-suspended in petri-dishes. In case the algae concentration was low the sample was concentrated and mixed thoroughly before analysis (Okolodkov, 1992, 1996).

The enumeration and identification of microalgae cells were carried out in 0.05-ml Naujotte counting chamber under a Zeiss Axioscope-40 non-inverted light microscope at a magnification of 100 - 400. If sufficient material was available > 300 cells were counted. The bio-volume was calculated from the volumes of appropriate stereometrical bodies (Hillebrand et al., 1999; Olenina et al., 2006). Taxa were identified to species level according to Medlin and Priddle (1990), Tomas et al. (1996), Bérard-Therriault et al. (2000), Gogorev et al. (2006). The ecological preferences of diatom and dinoflagellate species and their phytogeographical distribution were identified in accordance with Pankow (1990), Okolodkov and Dodge (1997), Okolodkov (2005), Polyakova (2003), and Poulin et al. (2011).

2.5. Remote Sensing, ice age reconstruction, and back-trajectories calculations

In this paper, we reconstruct the age and origin of fast ice in the vicinity of the sampling sites TI12_01_06 & _07, TI12_03_05 & _010 and TI12_02_07 using Environmental Satellite (ENVISAT) imagery. In total, 30 synthetic aperture radar (SAR) scenes were obtained over the south-eastern Laptev Sea between November 2011 and April 2012. The data are VV polarized with a spatial resolution of 150 m×150 m and a footprint of 400 km×400 km.

The fast ice age and origin as well as subsequent pathways of the sampled sites were determined by means of geographical information software (ArcGIS, ESRI). First, prominent fast ice features such as zones of homogenous backscatter that are likely to be of same age, were manually identified on SAR images obtained in March 2012. Then these zones were identified on the preceding images and thereby traced backward in time until they reach an area where intensive ice production took place. Thus the origin of ice formation and ice drift vectors were reconstructed.

3. Results

3.1. Sedimentological and biogeochemical properties of the sea ice core

Generally the ice core TI12_07 can be divided into four different sections in terms of SPM and phosphate concentrations, CDOM absorption and algal abundances (Fig. 3). Sea ice salinities varied between 8 and 4 in the older part (0–40 cm core depth) and around 4, so that the near steady state salinity value for sea ice was reached (Notz and Worster, 2008) in core sections > 60 cm core depth (Fig. 3).

Section 1 (0–10 cm) is influenced by surface processes, and was partly covered by snow. It is characterized by high salinity and low SPM and phosphate concentrations, CDOM absorption, and the absence of algae cells.

In the sediment-laden core Section 2 (10–70 cm) SPM concentrations varied between 57.3 and 144.1 mg l^{-1} with the maximum concentration at 30–40 cm core depth (Fig. 3). The SEM picture of one of the ice core filters with high SPM concentration is characterized by a constant background matrix of particles and valves of the planktonic diatom *Thalassiosira antarctica* (Fig. 4). The majority of the particles are smaller than 10 μm, only rarely exceeding 30–40 μm. The phosphate concentration reached its maximum of 6.4 μmol l^{-1}, which is an order of magnitude higher than the summer concentration in the Laptev Sea (0.5–1.4 μmol l^{-1}; Pivovarov et al., 2004) and the winter concentration in the Lena River (0.1–0.36 μmol l^{-1}, Arctic Great Rivers Observatory). Studies on first-year sea ice in the Sea of Okhotsk showed the same correspondence of sediment-laden layers and extremely high phosphate concentration considerably enriched compared to the seawater signal suggesting remineralization of the incorporated particulate organic matter (Nomura et al., 2010). Although the initial concentrations of CDOM and inorganic nutrients in the water column are not known, the results indicate that dissolved nutrients and CDOM, like the sea salt, are not completely removed from the ice during the freezing process. Nevertheless, seawater in the near-delta mixing zone (salinity ~5) usually shows CDOM absorptions that are an order of magnitude higher than the values that were measured in dirty sea ice of the same salinity (~7 m^{-1} vs. ~0.64 m^{-1} at 375 nm). The ice core further contained numerous and abundant freshwater diatoms, which are typical for the Lena River phytoplankton (*Aulacoseira islandica, A.italica* and others). They comprised 21.79 – 22.25% of total diatom abundances.

Section 3 (70–130 cm) is defined by low SPM and phosphate concentrations, CDOM absorption, and algal abundances.

Section 4 (130–180 cm) is the youngest part of the sea ice core and characterized by low SPM. Phosphate concentrations slightly increase up to 1.14 μmol l^{-1} at the ice-water interface, suggesting that the spring bloom started at the time of sampling. CDOM absorption increased probably due to autochthonous CDOM caused by high algal abundances. The algal abundances and biomass reached their maximum with up to 118.4 cells/ml and 18482.9 μg C ml^{-1}. The ice-associated species which were recorded in the lower part of the ice core (130–180 cm) are common in early-spring sea-ice communities in the Arctic region. All of these species belong to the same class (*Bacillariophyceae* or diatoms). Pennate diatoms (bilaterally symmetrical; *Pauliella taeniata, Navicula vanhoeffenii, Fragilariopsis oceanica, F. cylindrus, Nitzschia frigida, N. neofrigida, Fossula arctica, Haslea vitrea, Pseudogomphonema arcticum, Entomoneis kjelmanii*) dominated in the lower part of the ice core (> 70% of total biomass and abundance; Fig. 3b). They occurred as solitary cells or as ribbon-shaped colonies. The cell size (length) varied from 10 to 100 μm. The lowermost part of the core (170–180 cm) was characterized by a presence of typical Arctic early-spring marine planktonic species (*Thalassiosira nordenskioeldii, Chaetoceros socialis*). These are centric diatoms (radially symmetrical) which usually form colony consisting of several cells. The average cell size (width) was > 50 μm. The highest algae abundances and biomass is found in the lowermost part of this first-year sea ice core, which agrees well with previous sea-ice studies (e.g., Poulin et al., 1983; Syvertsen, 1991; Okolodkov, 1992, 1996; Melnikov, 1997; Melnikov et al., 2002).

3.2. Under-ice sediment dynamics

Generally the SPM concentrations in the upper 10 m of the water column were low with 0.3–1.1 mg l^{-1} (Fig. 5). Maximum concentrations of up to 10 mg l^{-1} were found near the seafloor in the bottom nepheloid layer (Fig. 5b). Turbidity meter measurements generally present similar patterns at the northernmost stations (TI12_01, _06, _09; Fig. 5b, e) with low turbidity in the upper water column and a pronounced layer of increased turbidity close to the bottom, characteristic for the 5–9 m thick bottom nepheloid layer. At the ice core stations
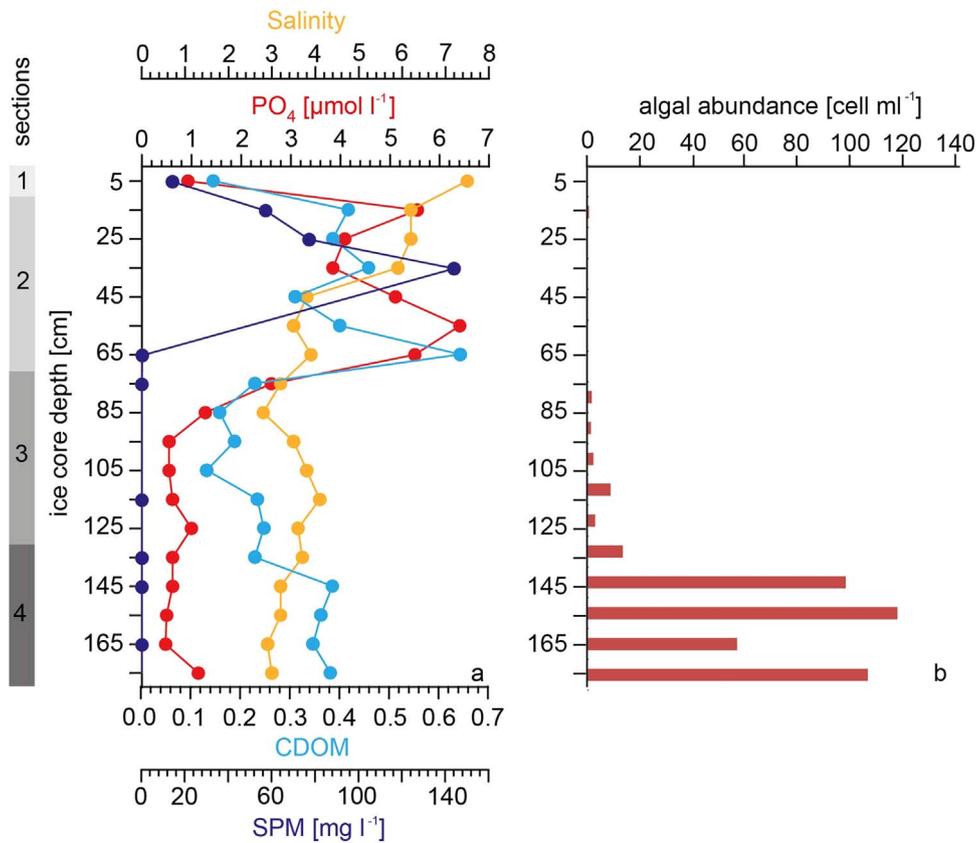
Fig. 3. (a) Salinity (orange), phosphate concentration (PO$_4$ [µmol l^{-1}], red), CDOM absorption at 375 nm ([m^{-1}], blue), SPM concentration ([mg l^{-1}], purple), and (b) algal abundances [cells ml^{-1}] in the ice core TI12_07. (For interpretation of the references to color in this figure legend, the reader is referred to the web version of this article.)
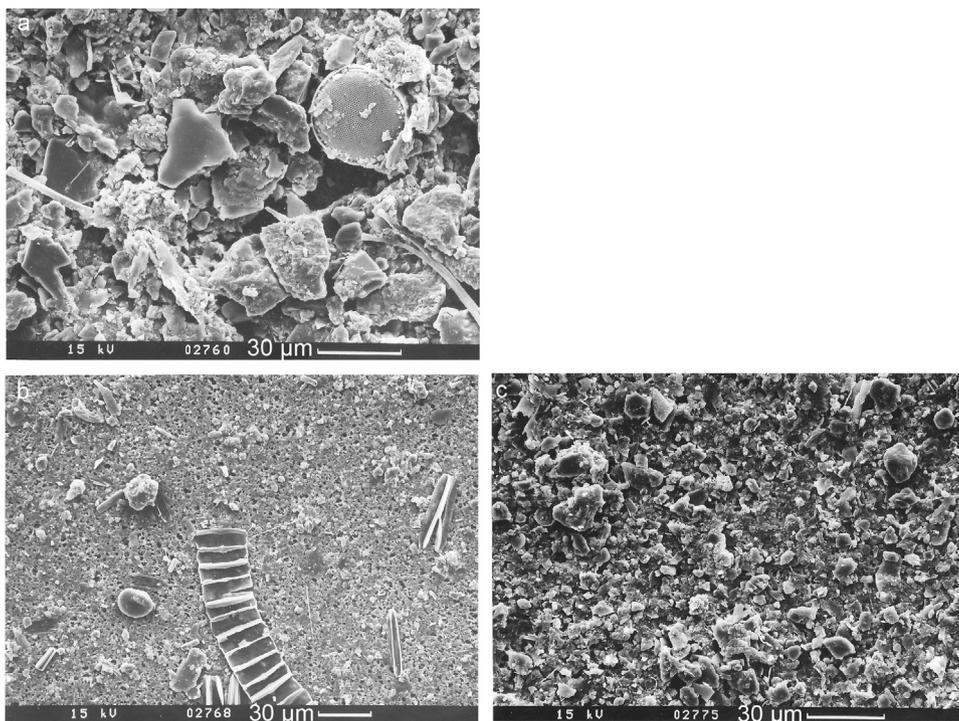
Fig. 4. Scanning electron microscope (SEM) pictures of (a) sea ice sample TI_12_07 from 10 to 20 cm core depth with a SPM concentration of 57.3 mg l^{-1}, water samples from (b) 2 m water depth just beneath the sea ice with a SPM concentration of 0.6 mg l^{-1}, and (c) from the bottom nepheloid layer in 17 m water depth with a SPM concentration of 10 mg l^{-1}.

(TI12_02, _07; Fig. 5c, f) the turbidity measurements revealed a bottom nepheloid layer as well as increased turbidity in the upper 2 m suggesting a slight influence of riverine waters (Fig. 5f), even though

salinity increased in the surface layer during the repeat-sampling of this station (TI12_02 & _07; Fig. 5f). The southernmost station (TI12_05, _10; Fig. 5a, d) did not show a bottom nepheloid layer at
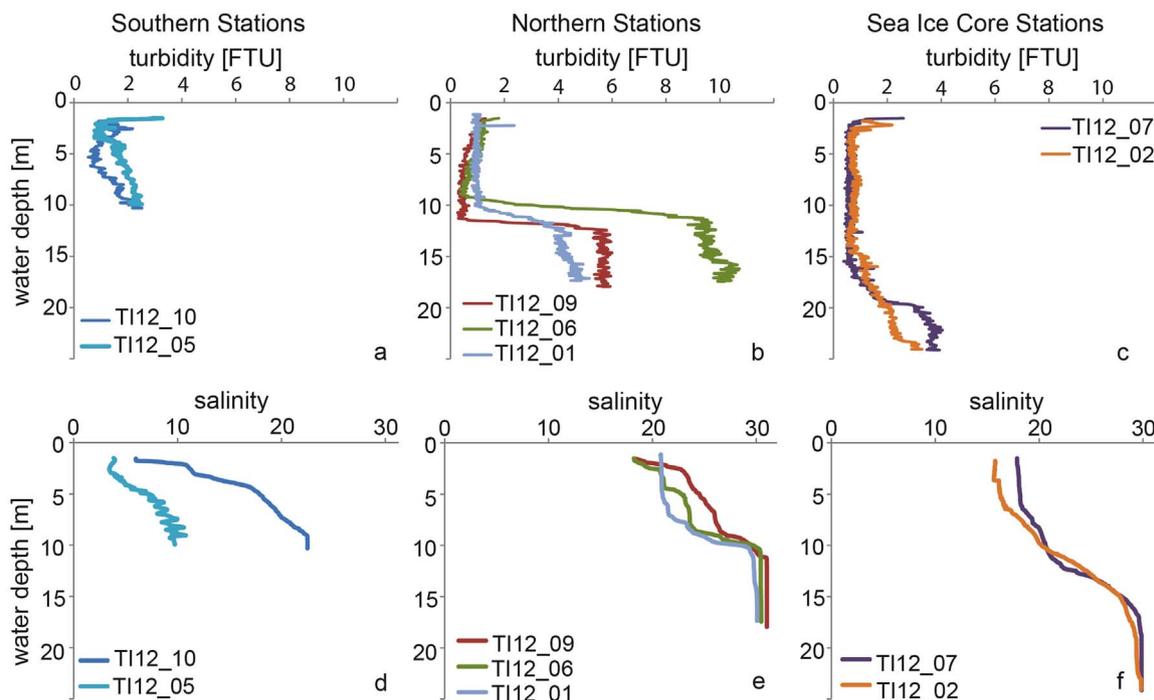
Fig. 5. Turbidity [FTU] and salinity distribution in the water column at the southern (a, d), the northern (b, e) and the sea ice core stations (c, f).

any time, but a layer of increased turbidity in the upper 2 m, suggesting a riverine influence.

Water sampling for the analysis of under-ice phytoplankton distribution at the ice core position was conducted twice on 27 March 2012 (TI_12_02) and 12 April 2012 (TI_12_07). Obtained results revealed an increase of the algal abundance in the water column. In the end of March (TI12_02; results not shown) only single cells of sea-ice diatoms (*Entomoneis kjelmanii, Nitzschia frigida, Pauliella taeniata*) and dinoflagellates (*Dinophysis acuminate, Protoperidinium ovatum*) were found in the upper water column (2–10 m). In the middle of April (TI12_07; Fig. 6a) total algae abundances was slightly higher (5.7 cells/l) compared to our March records. . Sea-ice diatoms (*Pauliella taeniata, Fragilariopsis oceanica, Nitzschia frigida*) dominated assemblages (75.3–100%) throughout all depths, which may be due to vertical mixing of the water column. In the uppermost layer (2 m) and in 15 m water depth algae assemblages contained freshwater, mainly riverine planktonic diatoms (*Aulacoseira italica, A. islandica*; Fig. 4b). The average particle size was ≤10 μm. SEM pictures from the bottom nepheloid layer in contrast were characterized by a constant matrix of 5 μm particles, reaching rarely 10 μm (Fig. 4c). The small amount of

diatom fragments belong to marine and freshwater species of *Thalassiosira, Aulacoseira* and *Cyclotella* genera (Fig. 4c), probably originating from the bottom sediments.

The acoustic record at Khatanga shows generally higher echo intensity corresponding with increased SPM concentration in the bottom nepheloid layer, while the echo intensity near the surface was low, suggesting very low SPM concentration in the upper water column (Fig. 7). In general the depth-averaged echo intensity decreased gradually from December 2011 until March 2012, and SPM dynamics slowed down. Beginning in mid-May 2012, the echo intensity in the near-surface layer suddenly increased, which may be indicative of riverine influence due to the high number of particles that are usually found in the Lena River plume (e.g. Wegner et al., 2005).

4. Discussion

Sediment entrainment into sea ice during autumn freeze up in the Siberian Arctic Shelf Seas is well documented in water depths of less than 20 m (Eicken et al., 1997; Hölemann et al., 1999a; Lindemann, 1999; Eicken et al., 2000). Modelling studies, laboratory experiments
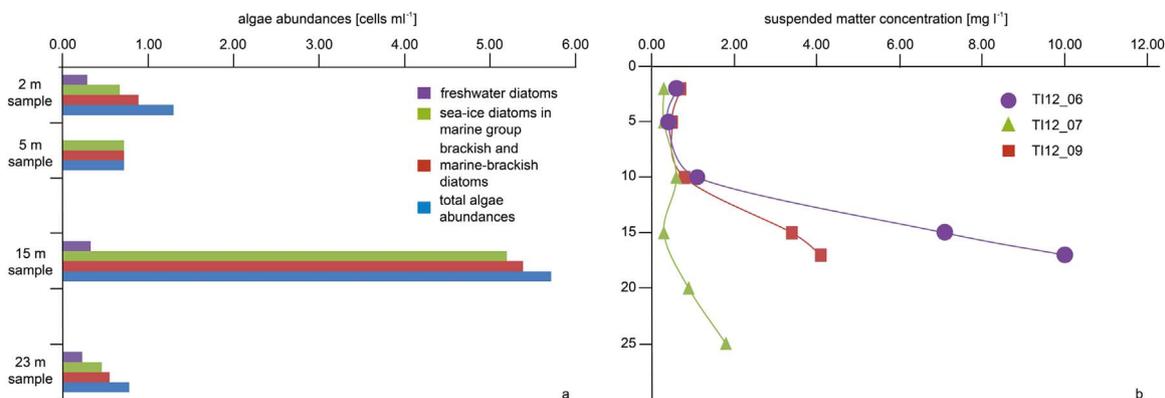
Fig. 6. (a) Total algae abundances [cells ml⁻¹] (blue), portion of freshwater diatoms (purple), of sea-ice diatoms in the marine group (green), and of the marine-brackish diatoms (red) beneath the sea-ice core (TI12_07); (b) SPM concentration [mg l⁻¹] from water samples from the northernmost station (TI12_06, purple, TI12_09, red), and sea ice core position (TI12_07, green). (For interpretation of the references to color in this figure legend, the reader is referred to the web version of this article.)
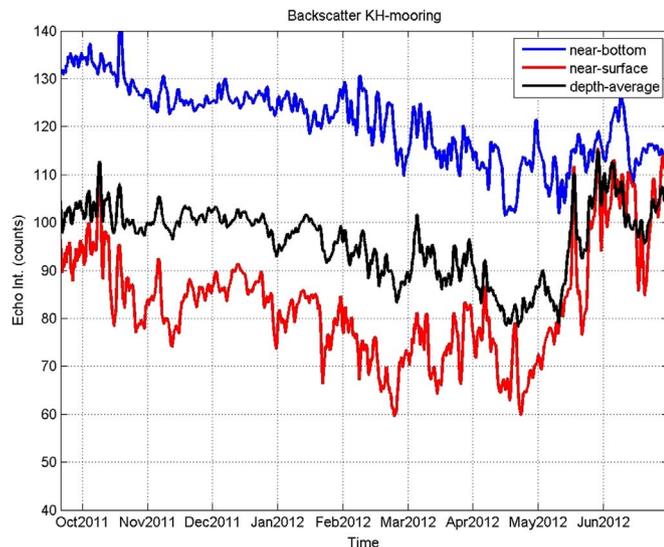
Fig. 7. Echo intensity at the 43 m-deep long-term mooring from October 2011 to June 2012 near the bottom (37–39 m water depth; blue), near the surface (3–7 m water depth; red), and depth averaged (black) with generally higher intensities and therefore higher SPM concentration in the bottom nepheloid layer. The depth-averaged echo intensity decreased gradually from December 2011 until March 2012, because material partly settled and SPM dynamics slowed down. The distinct increase in mid-May 2012 might be related to the riverine influence. (For interpretation of the references to color in this figure legend, the reader is referred to the web version of this article.)

and field observations (Sherwood, 2000; Smedsrud, 2003) have shown that wave-induced turbulence and sediment resuspension in combination with freezing in unstratified waters are essential requirements for sediment entrainment into newly formed sea ice. The Laptev Sea has as much as 1000 km of fetch at the end of summer, when freezing storms move in and large waves can form. In addition, during early winter (October-December), the polynya is maintained in the vast sediment-laden near-shore waters between the coast and the ~10 m-isobath (Reimnitz et al., 1994) and thus provides ideal conditions for sediment entrainment.

Based on theoretical considerations it was proposed that sediment suspension freezing can also take place in winter polynyas in water depths between 20 and 30 m (Dethleff, 2005). However, while mooring-based observations from the Laptev Sea shelf did indicate frazil ice formation, they did not show any sediment incorporation within the West New Siberian Polynya region in water depths of ~25 m (Dmitrenko et al., 2010) probably due to missing SPM at those depths where frazil ice forms. At the long-term mooring Khatanga peaks in echo intensity in the bottom nepheloid layer were not reflected in the surface layer (Fig. 7) indicating that upward-mixing of material was not taking place. Earlier studies on winter sediment dynamics on the Laptev Sea shelf highlighted events of bottom-sediment resuspension and transport within the West New Siberian Polynya, but no upward mixing of material in the upper water column (Wegner et al., 2005). As data from long-term mooring deployments in mid-shelf polynyas (water depth > 20 m) provide no indication of sediment entrainment, the formation of sediment-laden sea ice in shallow coastal areas during the first month of winter seems to be the dominant process that leads to the formation of sediment-laden sea ice in the Laptev Sea. Unfortunately, the majority of sea ice that formed during early winter in the coastal area is already far off shore at the end of winter (Krumpen et al., 2013) and therefore out of range for helicopter based expeditions which require daylight due to safety regulations. Therefore sediment-laden sea ice from near-shore polynyas that is eventually incorporated into the immobile fast ice belt provides an excellent opportunity to study the sediment entrainment process in near-shore polynyas.

Sea ice back-trajectories indicate a shallow (~10 m) near-shore area close to one of the main outlets of the Lena River as a potential source region for the sampled sea ice (Fig. 8) in this study. Based on a reconstructed sea ice age of 92 days (Fig. 8) its formation time was around 5 December 2011. SAR images from December 5–10, 2011 show a period when the fast ice opened near the main Lena River outlet and frazil ice formation took place (Fig. 9). Due to prevailing westerly winds with speeds > 15 m s^{-1} (Fig. 2a) the open water area enlarged and new ice formation continued until December 10, 2011 (Fig. 9b). These high wind speeds are within one standard deviation of the long-term mean during this time of year (Fig. 2b), suggesting that near-
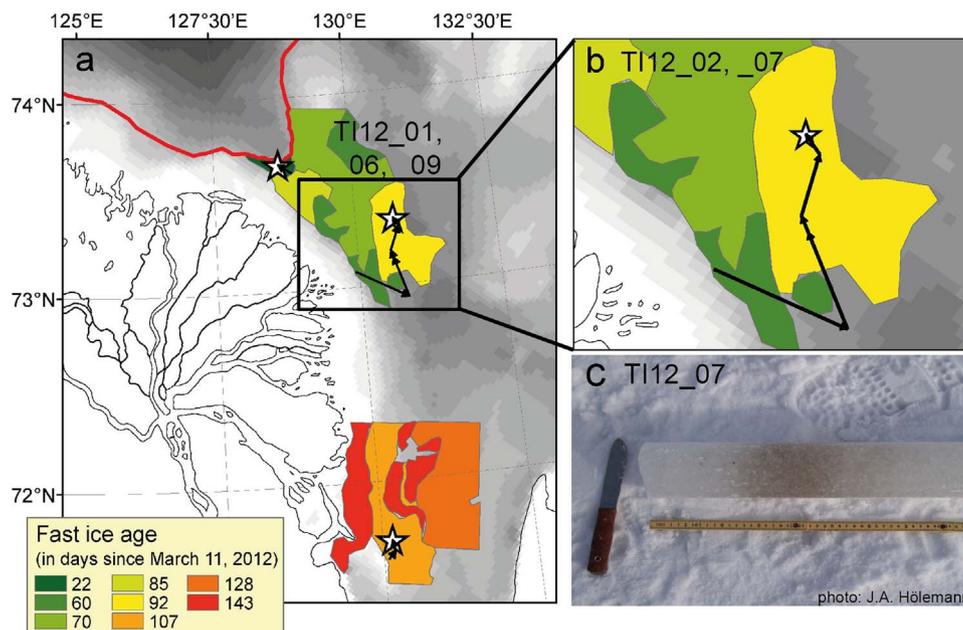
Fig. 8. Fast ice age and sea-ice drift reconstructions for the entire TRANSDRIFT XX region with the red line marking the fast ice edge during the expedition (a), details for the ice core position (b) and a photograph of the sampled ice core at TI12_07 (c). (For interpretation of the references to color in this figure legend, the reader is referred to the web version of this article.)
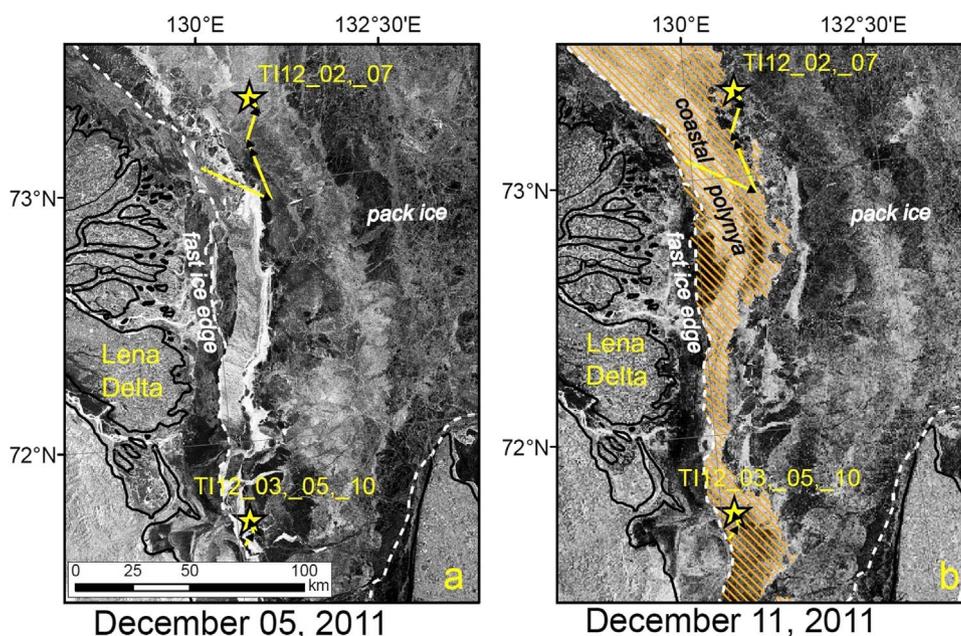
Fig. 9. ENVISAT SAR scene of the eastern Laptev Sea shelf from December 5, 2011 (a), showing a very narrow strip of fast ice along the Lena Delta coast and the pack ice zone east of the fast ice edge. The scene from December 10, 2011 (b) additionally shows an open-water area with new ice formation (coastal polynya) in the potential formation area of the sea ice core (TI12_07) between the fast ice and the pack ice zone east of the fast ice edge. The striped area represents the open water area used for sea ice formation estimates.

shore polynya events such as the one described in this study might be quite common during prevailing westerly winds. The water depth in the specific formation area is about 10 m and shallow enough that waves and/or wind-induced currents could have resuspended sediments.

As surface waves are a function of fetch and wind speed, the potential wave height generally deceases with wind fetch (Pavlov, 1996; Lintern et al., 2013). However, studies within the potential source area during freeze-up in October 1995 with calm weather conditions and mean wave heights of 1 m (Lindemann et al., 1999) found SPM concentrations in sea ice up to 250 mg l^{-1}, with a median SPM content of 149 mg l^{-1} (Lindemann et al., 1999). These numbers are similar to the maximum content found after the nearshore ice-formation event described in this study that occurred much later in the year than in 1995. After its formation, the sea ice drifted about 85 km to the sampling area.

The sediments in sea ice core Section 2 cover a wide range of grain sizes with particles of up to 30 μm and fresh water diatoms (Fig. 4), which might be related to the bottom material in the source area. The dominant particle size of 5–10 μm comprises the typical range for SPM (Dethleff and Kuhlmann, 2010). Sections 3 and 4 of the sea ice core can be related to the period of ice growth during drift (Fig. 3).

We estimated a maximum open water area of 7630 km^2 (Fig. 9b) for the nearshore polynya event in December 2011 for 3–5 days. The ice growth rate calculated from a simple freezing degree days model results in the formation of 12–19 cm of ice during this period. Assuming a mean SPM content in the newly formed ice of 91.9 mg l^{-1} suggests that 8.4×10^4 - 1.3×10^5 t of sediments might have been incorporated into sea ice in this polynya. Extrapolating these sediment loads for the entire Lena Delta region suggests that about 3.9×10^5 t could be incorporated during such an event and subsequently transported onto the outer shelf or even off-shelf. This sediment load would be 65% of the minimum estimated sediment loads of 6×10^5 t (Lindemann, 1998) to be incorporated during freeze-up and 9.8% of sediments to be exported annually off the Laptev Sea shelf (roughly 4×10^6 t; Eicken et al., 1997, 2000). Nearshore polynya events such as the one described in this paper might therefore contribute significantly to the sediment export into the deep Arctic Ocean. However, the contribution of these events on the sediment budget across the Arctic

Ocean into Fram Strait might be small during years of high winter ice export, when the exported ice cover is generally thinner (Krumpen et al., 2013) and therefore melts faster and might hence release sediments earlier within the Transpolar Drift.

5. Summary and conclusions

A sediment-laden sea ice core was sampled during a helicopter-based expedition to the Laptev Sea in March/April 2012, which allowed for new insights regarding the incorporation of sediments into sea ice during winter. Sedimentological (SPM concentration, SEM analysis), biogeochemical (CDOM absorption, nutrients) and biological (algal abundances) studies on the ice core in combination with satellite images and ice drift back-trajectories allowed to reconstruct the formation process and area. The sediments were found in the upper part of the core (10–70 cm, Fig. 3) along with abundant freshwater diatoms typical for Lena River phytoplankton and further with max-imum phosphate concentrations being an order of magnitude higher than Laptev Sea summer and the Lena River winter concentrations. The sediments were incorporated near the shallow (10 m) Lena Delta during a nearshore polynya event, caused by westerly winds of > 15 m s^{-1} (Fig. 2). The event likely caused wave- or current-induced resuspension of bottom sediments, which were then incorporated into frazil ice and transported ~ 80 km northeastward onto the shelf (Fig. 8). Complementary fast ice-based water column and oceano-graphic process studies near the Lena Delta and the West New Siberian Polynya during March/April 2012 found no evidence for sediment incorporation into sea ice near polynyas, but instead showed near-bottom matter transport beneath the sea ice during winter. The event lasted for 4 days and affected an area of ~ 7630 km^2 and results in an estimated total sediment incorporation of 8.4×10^4 - 1.3×10^5 t, which suggests that these events provide a significant contribution to the variability of the Laptev Sea's sediment budget.

Studies on the Chukchi and Beaufort shelves (Eicken et al., 2005) suggest an increase of sediment entrainment into sea ice in late winter due to changes in the sea ice regime towards more frequent mid-winter breakup events. If a similar trend existed on eastern Arctic shelves, an increase in the occurrence of sediment-laden ice can be expected in the

Laptev Sea as well, which might then impact the regional sediment budget and further have consequences for radiation balance within the export pathways of the Laptev Sea ice in the Transpolar Drift.

References

Bareiss, J., Görgen, K., 2005. Spatial and temporal variability of sea ice in the Laptev Sea: analyses and review of satellite passive-microwave data and model results, 1979 to 2002. Glob. Planet. Change 48, 28–54. http://dx.doi.org/10.1016/j.gloplacha.2004.12.004.

Bérard-Therriault, L., Poulin, M., Bossé, L., 2000. Guide d'indentification du phytop;ancton marin de l'estuare et du golfe du Saint-Laurent: incluant également certains protozoaires. Canadian Special Publication of Fisheries and Aquatic Sciences. Publisher NRC Research Press, Ottawa, Canada, 387.

Comiso, J.C., Parkinson, C.L., Gersten, R., Stock, L., 2008. Accelerated decline in the Arctic sea ice cover. Geophys. Res. Lett. 35, L01703. http://dx.doi.org/10.1029/2007GL031972.

Darby, D.A., Myers, W.B., Jakobsson, M., Rigor, I., 2011. Modern dirty sea ice characteristics and sources: the role of anchor ice. J. Geophys. Res. 116, C09008. http://dx.doi.org/10.1029/2010JC006675.

Dethleff, D., 2005. Entrainment and export of Laptev Sea ice sediments, Siberian Arctic. J. Geophys. Res. 110, C07009. http://dx.doi.org/10.1029/2004JC002740.

Dethleff, D., Kempema, E.W., 2007. Langmuir circulation driving sediment entrainment into newly formed ice: tank experiment results with application to nature (Lake Hattie, United States; Kara Sea, Siberia). J. Geophys. Res. 112, C02004. http://dx.doi.org/10.1029/2005JC003259.

Dethleff, D., Kuhlmann, G., 2010. Fram Strait sea-ice sediment provinces based on silt and clay compositions identify Soberian Kara and Laptev Sea seas as main source regions. Polar Res. 29, 265–282. http://dx.doi.org/10.1111/j.1751-8369.2010.00149.x.

Dethleff, D., Rachold, V., Tintelnot, M., Antonow, M., 2000. Sea-ice transport of riverine particles from the Laptev Sea to Fram Strait based on clay mineral studies. Int. J. Earth Sci. 89, 496–502.

Dmitrenko, I., Wegner, C., Kassens, H., Kirillov, S., Krumpen, T., Heinemann, G., Helbig, A., Schröder, D., Hölemann, J.A., Klagge, T., Tyshko, K.P., Busche, T., 2010. Observations of supercooling and frazil ice formation in the Laptev Sea coastal polynya. J. Geophys. Res. 115, C05015. http://dx.doi.org/10.1029/2009JC005798.

Eicken, H., Reimnitz, E., Alexandrov, V., Martin, T., Kassens, H., Viehoff, T., 1997. Sea-ice processes in the Laptev Sea and their importance for sediment export. Cont. Shelf Res. 17 (2), 205–233.

Eicken, H., Kolatschek, J., Freitag, J., Lindemann, F., Kassens, H., Dmitrenko, I., 2000. A key source area and constraints on entrainment for basin-scale sediment transport by Arctic sea ice. Geophys. Res. Lett. 27 (13), 1919–1922.

Eicken, H., Gradinger, R., Gaylord, A., Mahony, A., Rigor, I., 2005. Sediment transport by sea ice in the Chuckchi and Beaufort Seas: increasing importance due to changing ice conditions? Deep-Sea Res. II 52, 3281–3302. http://dx.doi.org/10.1016/j.dsr2.2005.10.006.

Gogorev, R.M., Orlova, T., Yu, Shevchenko, O.G., Stonik, I.V., 2006. Diatoms of Russia and adjacent countries: fossil and recent. In: Strelnikova, N.I. (Ed.), Chaetocerotales (Chaetocerotaceae, Acanthocerataceae, Attheyaceae) Vol. II. St. Petersburg University Press, 180, (in Russian).

Hillebrand, H., Durselen, C.D., Kirschtel, D., Pollingher, U., Zohary, T., 1999. Biovolume calculation for pelagic and benthic microalgae. J. Phycol. 35, 403–424.

Hölemann, J.A., Schirmacher, M., Kassens, H., Prange, A., 1999a. Geochemistry of surficial and ice-rafted sediments from the Laptev Sea (Siberia). Estuar. Coast. Shelf Sci. 49, 45–59.

Hölemann, J.A., Schirmacher, M., Prange, A., 1999b. Dissolved and particulate major and trace elements in newly formed ice from the Laptev Sea (Transdrift III, October 1995). In: Kassens, H., Bauch, H.A., Dmitrenko, I., Eicken, H., Hubberten, H.-W., Melles, M., Thiede, J., Timokhov, L. (Eds.), Land-Ocean Systems in the Siberian Arctic: Dynamics and History. Springer-Verlag, Berlin, 101–111.

Hölemann, J.A., Kirillov, S., Klagge, T., Novikhin, A., Kassens, H., Timokhov, L., 2011. Near-bottom water warming in the Laptev Sea in response to atmospheric and sea ice conditions in 2007. Polar Res. 30, 6425. http://dx.doi.org/10.3402/polar.v30i0.6425.

Janout, M.A., Hölemann, J., Krumpen, T., 2013. Cross-shelf transport of warm and

saline water in response to sea ice drift on the Laptev Sea shelf. J. Geophys. Res. Oceans 118, 563–576. http://dx.doi.org/10.1029/2011JC007731.

Junge, K., Eicken, H., Deming, J.W., 2004. Bacterial activity at -2 to -20 °C in Arctic winter time sea ice. Appl. Environ. Microbiol. 70, 550–557.

Kempema, E.W., Reimnitz, E., Barnes, P.W., 1989. Sea ice sediment entrainment and rafting in the Arctic. J. Sediment. Res. 59 (2), 308–317.

Krumpen, T., Janout, M., Hodges, K.I., Gerdes, R., Girard-Arduhin, F., Hölemann, J.A., Willmes, S., 2013. Variability and trends in the Laptev Sea outflow between 1992–2011. Cryosphere 7, 349–363. http://dx.doi.org/10.5194/tc-7-349-2013.

Kwok, R., Cunningham, G.F., Wensnahan, M., Rigor, I., Zwally, H.J., Yi, D., 2009. Thinning and volume loss of the Arctic Ocean sea ice cover: 2003–2008. J. Geophys. Res. 114, C07005. http://dx.doi.org/10.1029/2009JC005312.

Lindemann, F., Hölemann, J.A., Korablev, A., Zachek, A., 1999. Particle entrainment into newly forming sea ice – freeze-up studies in October 1995. In: Kassens, H., Bauch, H.A., Dmitrenko, I., Eicken, H., Hubberten, H.-W., Melles, M., Thiede, J., Timokhov, L. (Eds.), Land-Ocean Systems in the Siberian Arctic: Dynamics and History. Springer-Verlag, Berlin, 113–123.

Lindemann, F., 1998. Sediments in Arctic sea ice – entrainment, characterization and quantification. Reports on Polar Research 283, 1-124 (in German).

Lintern, D.G., Macdonald, R.W., Solomon, S.M., Jakes, H., 2013. Beaufort Sea storm and resuspension modeling. J. Mar. Syst. 127, 14–25. http://dx.doi.org/10.1016/j.jmarsys.2011.11.015.

Mahoney, A.R., Barry, R.G., Smolyanitsky, V., Fetterer, F., 2008. Observed sea ice extent in the Russian Arctic, 1933–2006. J. Geophys. Res. 113, C11005. http://dx.doi.org/10.1029/2008JC004830.

Maslanik, J.A., Fowler, C., Stroeve, J., Drobot, S., Zwally, J., Yi, D., Emery, W., 2007. A younger, thinner Arctic ice cover: increased potential for rapid, extensive sea-ice loss. Geophys. Res. Lett. 34, L24501. http://dx.doi.org/10.1029/2007GL032043.

Medlin, L.K., Priddle, J. (Eds.), 1990. Polar Marine Diatoms. British Antarctic Survey. Natural Environment Research Council, Cambridge, UK, 214.

Melnikov, I.A., 1997. The Arctic Sea Ice Ecosystem. Gordon and Breach Science Publishers, 204.

Melnikov, I.A., Kolosova, E.G., Welch, H.E., Zhitina, L.S., 2002. Sea-ice biological communities and nutrient dynamics in the Canada Basin of the Arctic Ocean. Deep-Sea Res. I 49, 1623–1649.

Nomura, D., Nishioka, J., Granskrog, M.A., Krell, A., Matoba, S., Toyota, T., Hattori, H., Shirasawa, K., 2010. Nutrient distributions associated with snow and sediment-laden layers in sea ice of the southern Sea of Okhotsk. Mar. Chem. 119, 1–8. http://dx.doi.org/10.1016/j.marchem.2009.11.005.

Notz, D., Worster, M.G., 2008. In situ measurements of the evolution of young sea ice. J. Geophys. Res. 113, C03001. http://dx.doi.org/10.1029/2007JC004333.

Okolodkov, Y.B., 1992. Cryopelagic flora of the Chukchi, East Siberian and Laptev seas. Proceedings of the National Institute of Polar Research Symposium on Polar Biology 5, 28-43.

Okolodkov, Yu, 2005. The global distributional patterns of toxic, bloom dinoflagellates recorded from the Eurasian Arctic. Harmful Algae 4, 351–369. http://dx.doi.org/10.1016/j.hal.2004.06.016.

Okolodkov, Yu, Dodge, J.D., 1997. Morphology of some rare and unusual dinoflagellates from the north-eastern Atlantic. Nova Hedwig. 64 (3–4), 353–365.

Okolodkov, Yu.B., 1996. Vertical distribution of algae and nutrients in the first-ear ice from the East Siberian Sea in May 1987. Bot. J. Russ. Acad. Sci. 81 (7), 34–40.

Olenina, I., Hajdu, S., Edler, L., Andersson, A., Wasmund, N., Busch, S., Göbel, J., Gromisz, S., Huseby, S., Huttunen, M., Jaanus, A., Kokkonen, P., Ledaine, I., Niemkiewicz, E., 2006. Biovolumes and size-classes of phytoplankton in the Baltic Sea. HELCOM Balt. Sea Environ. Proc. 106, 1–144.

Pankow, H., 1990. Ostsee-Algenflora. Gustav Fischer Verlag, Jena, 648.

Pavlov, V.K., Timokhov, L.A., Baskakov, G.A., Kulakov, M.Y., Kurazhov, V.K., Pavlov, P.V., Pivovarov, S.V., Stanvoy, V.V., 1996. Hydrometeorological regime of the Kara, Laptev, and Eats Siberian seas. Technical Memorandum APL-UW TM1-96. University of Washington, 179.

Pivovarov, S.V., Hölemann, J.A., Kassens, H., Piepenburg, D., Schmidt, M.K., 2004. Laptev and East Siberian Seas. In: Robinson, R.A., Brink, K.H. (Eds.), The Sea 14, Part B. Harvard University Press, 1107–1133.

Polyak, L., Alley, R.B., Andrews, J.T., Brigham-Grette, J., Cronin, T.C., Darby, D., Dyke, A.S., Fitzpatrick, J.J., Funder, S., Holland, M., Jennings, A.E., Miller, G.H., O'Regan, M., Savelle, J., Serreze, M., St., John, K., White, J.W.C., Wolff, E., 2010. History of sea ice in the Arctic, Quaternary Science Review. 29 (15–16), 1757–1778. http://dx.doi.org/10.1016/j.quascirev.2010.02.010.

Polyakova, Ye.I., Diatom assemblages in surface sediments of the Kara Sea (Siberian Arctic) and their relationship to oceanological conditions. 2003. In: Siberian river run-off in the Kara Sea. In: Stein, R., Fahl, K., Fütterer, D.K., Galimov, E.M., Stepanets, O.V., (eds.). Proceedings in Marine Science 6, 375-400.

Poulin, M., Cardinal, A., Legendre, L., 1983. Réponse d'une communauté de diatomées de glace á un gradient de salinité(baie d'Hudson). Mar. Biol. 76, 191–202.

Poulin, M., Daugbjerg, N., Gradinger, R., Ilyash, L., Ratkova, T., von Quillfeldt, C., 2011. The pan-Arctic biodiversity of marine pelagic and sea-ice unicellular eukaryotes: a first-attempt assessment. Mar. Biodivers. 41, 13–28.

Reimnitz, E., Marincovich, L., Jr, McCormick, M., Brigs, W.M., 1992. Suspension freezing of bottom sediment and biota in the Northwest Passage and implications for Arctic Ocean sedimentation. Can. J. Earth Sci. 29, 693–703.

Reimnitz, E., Dethleff, D., Nürnberg, D., 1994. Contrasts in arctic shelf sea-ice regimes and some implications: beaufort Sea versus Laptev Sea. Mar. Geol. 119, 215–255.

Serreze, M.C., Holland, M.M., Stroeve, J., 2007. Perspectives on the Arctic's shrinking sea-ice. Science 315, 1533–1536.

Sherwood, C.R., 2000. Numerical model of frazil ice and suspended sediment concentrations and formation of sediment-laden ice in the Kara Sea. J. Geophys. Res.

105, 14061–14080.

Smedsrud, L.H., 2003. Formation of turbid ice during autumn freeze-up in the Kara Sea. Polar Res. 22 (2), 267–286.

Smedsrud, L.H., Sirevaag, A., Kloster, K., Sorteberg, A., Sanven, S., 2011. Recent wind driven high sea ice export in the Fram Strait contributes to Arctic sea ice decline. Cryosphere 5, 821–829. http://dx.doi.org/10.5194/tc-5-821-2011.

Spreen, G., Kwok, R., Menemenlis, D., 2011. Trends in Arctic sea ice drift and role of wind forcing: 1992–2009. Geophys. Res. Lett. 38, L19501. http://dx.doi.org/10.1029/2011GL048970.

Syvertsen, E.E., 1991. Ice algae in the Barents Sea: types of assemblages, origin, fate and role in the ice edge phytoplankton bloom. In: Sakshaug. E., Hopkins, C. C. E., Oritsland. N. A. (eds.): Proceedings of the Pro Mare Symposium on Polar Marine Ecology, Trondheim, 12-16 May 1990. Polar Research 10, 1, 277-287.

Tomas, C., Hasle, G.R., Syvertsen, E.E., Steidinger, K.A., Jangen, K. (Eds.), 1996. Identifying Marine Diatoms and Dinoflagellates. Academic Press, 598.

Wegner, C., Hölemann, J.A., Dmitrenko, I., Kirillov, S., Kassens, H., 2005. Seasonal variations in sediment dynamics on the Laptev Sea shelf (Siberian Arctic). Glob. Planet. Change 48, 126–140.

Zakharov, V.F., 1966. The role of flaw leads off the edge of fast ice in the hydrological and ice regime of the Laptev Sea. Oceanology 6 (1), 815–821.